

A representative template of the neonatal cerebellum

Carlos R. Hernandez-Castillo^{a,*}, Catherine Limperopoulos^b, Jörn Diedrichsen^{a,c}

^a Brain and Mind Institute, Western University, London, ON, Canada

^b Center for the Developing Brain, Advanced Pediatric Brain Imaging Research, Children's National Health System, Washington D.C., USA

^c Department of Computer Science and Department of Statistical and Actuarial Sciences, Western University, London, ON, Canada

ARTICLE INFO

Keywords:

Normalization
Cerebellum
Neonate
Developmental MRI

ABSTRACT

The cerebellum plays an important role in human brain development. To improve the spatial specificity of the analysis of human cerebellar magnetic resonance imaging (MRI) data, we present a new template of the neonatal human cerebellum and brainstem based on the anatomy of 20 full-term healthy neonates. The template is spatially unbiased, which means that the location of each structure is not biased by the anatomy of the individuals used to create the template. In comparison to current whole-brain templates, it allows for an improved voxel-by-voxel normalization for MRI analysis. To align the cerebellum to the template, it needs to be isolated from the surrounding tissue, a process for which an automated algorithm has been developed. Our methodology outperforms normalization to a whole-brain neonatal template, using either linear or nonlinear transformations. Our algorithm reduces the spatial variability of the infratentorial area, while simultaneously increasing the overlap of the cerebellum. The template and the related software are freely available as part of SUIT v3.3 SPM toolbox.

1. Introduction

The human cerebellum is an important part of brain development. The cerebellum is one of the first brain structures to differentiate, but one of the last to mature. It shows a growth rate that is unparalleled elsewhere in the brain (Triulzi et al., 2005). The maximum rate of growth occurs between 28 and 40 weeks of gestation, during which the cerebellar volume increases 5-fold, and it continues to grow for several years after birth (du Plessis et al., 2018; Volpe, 2009). Cerebellar injuries suffered during the premature period (e.g. hemorrhage, infarction, hypoxia, ischemia, etc.) potentially result in developmental disturbances that include deficits in motor planning and execution (Allin et al., 2001), cognitive impairment in verbal fluency, memory and learning (Limperopoulos et al., 2007), attentional shifting, or social/affective disturbances such as mood disorders or autistic spectrum disorders (Stoodley and Limperopoulos, 2016). Functionally, the cerebellum is extremely heterogeneous, supporting motor, cognitive and social functions in the adult brain. Therefore, the impact of pre- or perinatal abnormalities or lesions will differ substantially depending on their exact spatial location. While magnetic resonance imaging (MRI) is an important evaluation and possible prognostic tool in the neonatal period, the identification of at-risk newborn infants, especially those who would benefit from early intervention therapies, remains a challenge.

Neonatal MRI has been used to assess brain development (Gao et al., 2015; Knickmeyer et al., 2008) and damage in different groups of neonates, including both preterm and term-born infants (Triulzi et al., 2005; Volpe, 2009; Woodward et al., 2006). Despite the known importance of the cerebellum for development, few studies have investigated cerebellar abnormalities in neonates, as compared to cortical injuries (du Plessis et al., 2018). One important factor that contributes to this difference is the difficulty in analyzing cerebellar data. Compared to an adult structural MRI, neonatal images have inverted and low tissue contrast due to early myelination, resulting in the failure of automated segmentation algorithms when applied to neonate brains. In practice, researchers need to manually segment brain structures, a tedious and time consuming task. This problem scales up for group analysis using big data cohorts. For this reason, current reports show total cerebellar volume rather than computing voxel-by-voxel volumetry (ten Donkelaar et al., 2003). To date, few neonatal templates have been developed (Hashioka et al., 2012; Kazemi et al., 2007; Shi et al., 2011), and in some cases the cerebellum has even been removed to increase the accuracy of cortical alignment (Shi et al., 2011).

One problem for cerebellar normalization using a whole brain template, is that structural variability in the neocortex can induce inaccuracies in the alignment of the posterior fossa. This normalization problem is even more evident in neonates, since differences across certain weeks

* Corresponding author. 1151 Richmond St., Brain and Mind Institute, Natural Sciences Centre, Western University, London, Ontario, N6A 5B7, Canada.
E-mail address: chern3@uwo.ca (C.R. Hernandez-Castillo).

of gestation elicits differences in the size and maturation of the cerebellum. Isolating the cerebellum from the rest of the brain before normalization has been shown to improve the accuracy of alignment of cerebellar structures in the adult human brain (Diedrichsen, 2006; Diedrichsen et al., 2011). Therefore, a specialized tool to systematically assess this variability and to accurately normalize the neonatal cerebellum to an unbiased spatial template is critically needed in the growing field of neonatal imaging.

Here, we present a spatially unbiased cerebellar template for human neonates and the software to isolate and normalize the neonatal cerebellum. The Spatially Unbiased Infratentorial Template of the Neonatal cerebellum (SUIT-N) template and software are freely available as part of SUIT v3.3.

2. Materials and methods

2.1. Participants

The sample was comprised of twenty-five newborn infants with a mean gestational age of 40.2 weeks (SD 2.7). The study was approved by the institutional review board of the Children's National Hospital. Healthy neonates were recruited from Children's National Health System as controls in an ongoing prospective study examining brain development in fetuses and infants with congenital heart disease. Exclusion criteria were as follows: any dysmorphic features by antenatal ultrasound, chromosomal abnormalities by amniocentesis, multiple gestations, and evidence of congenital infection. Study participants were recruited between 2012 and 2016, and written informed consent forms were obtained from all the parents.

2.2. MRI protocol

All newborns underwent a MRI on a 3 T GE Healthcare Discovery MR750 scanner (Milwaukee, WI) with a 32-channel receive-only head coil (MR Instruments, Inc, Minneapolis, Minnesota). All MRI data acquisition was performed during natural sleep. Newborns were fed, swaddled, and immobilized using a newborn vacuum pillow (Newmatic Medical, Caledonia, MI). Silicone ear plugs and adhesive mini muffs were used for ear protection. A radiology nurse was present during the MRI scan to monitor vital signs. An anatomical T2-weighted sequence (3D Cube) was acquired as follows: echo/repetition time = 65/2500 ms, voxel size = $0.63 \times 1 \times 0.63$ mm, acquisition time = 3min 20s. All brain MRI studies were reviewed by an experienced pediatric neuroradiologist and were reported to have structurally normal brains and no motion artifacts.

2.3. MRI preprocessing

All images were resliced into left-posterior-inferior (LPI) orientation and the origin coordinate (0,0,0) was set into the anterior commissure. For the template construction, we used the images of 20 subjects, the other five were reserved as an independent data set to be used only in the final evaluation.

2.4. Isolation algorithm

Prior to normalization, the cerebellum was isolated from the surrounding tissue. Cerebellar and occipital gray matter have similar brightness values making a purely data-driven determination of the boundary between the visual cortex and the anterior cerebellum difficult. To overcome this problem, we used an iterative Bayesian algorithm that includes both segmentation and normalization, as implemented in SPM12 (Ashburner and Friston, 2005). The segmentation creates tissue probability maps of cerebellar gray-matter, cerebellar white-matter, and their cortical counterparts. The regular version of the unified segmentation in SPM12 uses priors for T1 weighted images of the adult brain. In

order to make the algorithm work in neonates we create a new set of priors using the T2 weighted images of 10 neonates. First, the T2 images were aligned to the UNC neonate template (Shi et al., 2011) using affine transformation. The aligned images were manually segmented into 7 tissue types (cerebellar gray matter, cerebellar white matter, cerebrospinal fluid, skull/fat/skin, air, cortical gray matter, and cortical white matter). For each tissue type, the average of the 10 images was calculated and used as a tissue probability maps. Then we used the modified algorithm to segment the neonatal data. The combination of cerebellar gray and white matter maps were used to create the cerebellar isolation mask. The final mask was binarized after erasing the voxels that had a probability smaller than 0.5 of belonging to cerebellar tissue. These isolation masks were then individually checked and manually corrected (if necessary) using MRICron software (<http://people.cas.sc.edu/rorden/mricron/index.html>).

2.5. Construction of the template

To generate a group template, the first step was to register the data of all subjects to a target. Usually the target is one specific subject. The disadvantage of this approach, however, is that the resultant template is not representative of the average cerebellar shape. Therefore, the amount of deformation applied to each subject must be taken into account to find the intermediate space, which is not biased towards any of the subjects in the sample. This process was described in detail in (Diedrichsen, 2006). Briefly, the generation of the template consisted of 5 steps. As described above, the T2 images (twenty subjects) were aligned using an affine transformation to the UNC template, segmented and the isolation mask was applied. Second, to avoid differences in the isolated cerebella intensities, we performed an intensity normalization by dividing every single image by its own robust maximum intensity (98th percentile). Third, subject 01 was selected as the target, and all images were normalized into the target using the technique developed by Ashburner et al. (Friston et al., 2007), and implemented as DARTEL in the SPM12 package. Fourth, the deformation vector of each individual was used to calculate the average deformation of the group. This vector points to a new space spatially unbiased with respect to the original group of individuals in UNC space. Fifth, we resampled the individual images into this new space using trilinear interpolation and averaged the resulting images. To guarantee convergence, the normalization process was repeated twice more, each time replacing the target image with the new cerebellar template.

2.6. Evaluation

To assess the general performance of our methodology, we compared SUIT-N with three commonly used whole-brain normalization methods: FSL FLIRT (linear), FSL FNIRT (nonlinear) and SPM12 normalize (nonlinear). To quantify the degree of anatomical overlap, we used two criteria: the voxel-by-voxel correlation between images and the spatial consistency of the cerebellar perimeter. The first measure consisted of calculating the pair-wise correlation between anatomical images after normalization using regular whole brain techniques or SUIT-N. The correlations were computed voxel-by-voxel within a mask spanning the cerebellum and brainstem plus a 1-cm rim around it. This method allows for the evaluation of both the internal overlap and the correspondence of the edges. In the second approach, we assessed the spatial spread of cerebellar and brainstem structures after normalization. We selected six slices of the raw T2 images (axial plane) in which the deep cerebellar nuclei were visible for every subject, and manually marked the cerebellar diameter. These marked images (individual perimeter masks) were resliced using the individual deformation fields resulting from each normalization process (FLIRT, FNIRT, Normalize, and SUIT-N). For each subject and method, we then determined the two points (one on each side of the image center) where the perimeter intersected the horizontal line at $z = -21$, $y = -35$ for the cerebellum and $z = -21$, $y = -18$ for the

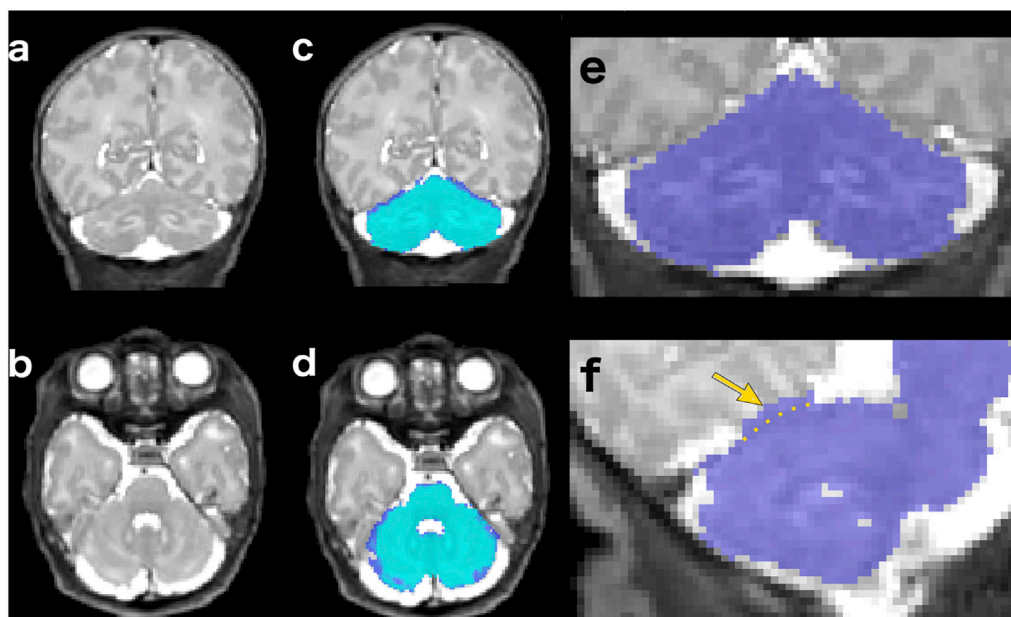


Fig. 1. Cerebellar isolation. (a) Coronal and (b) axial views of an example subject; (c) and (d) show the corresponding cerebellar posterior probabilities before binarization of the cerebellar mask. Lighter shade of blue indicates higher probability. (e) Shows the final mask and (f) a different subject (in sagittal view) in which voxels of the occipital cortex were mislabeled (yellow arrow).

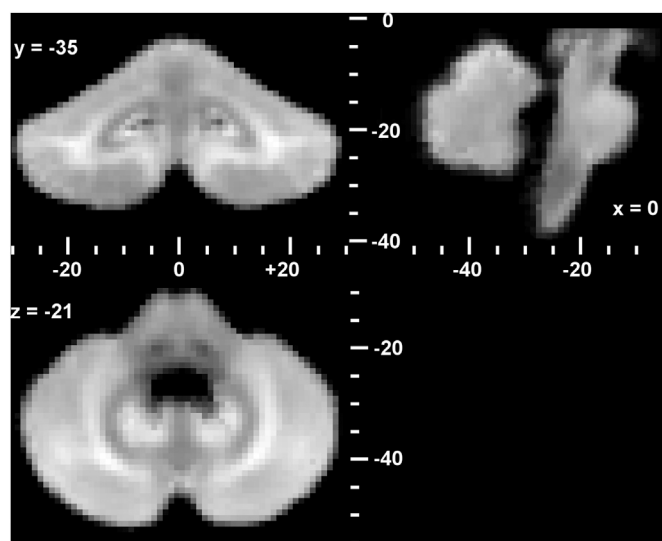


Fig. 2. Coronal, horizontal and sagittal view of the Spatially Unbiased Infratentorial Neonatal (SUIT-N) template. The coordinate system is defined by the UNC neonate template. The template image is based on the unbiased anatomy of 20 individuals (see methods).

brainstem. This plane ($z = -21$) corresponds to the place in the standard space for which the cerebellum is widest. As an evaluation criterion for size variability, we then calculated the SD of the individual cerebellar widths. To assess location variability, we determined the SD of the x-coordinate of the left and right intersection point. These measures were then averaged across sides. This metric is sensitive to a spatial misplacement of the perimeter even if the width is consistent. To avoid a possible increase in performance due to using the same data in both creation and evaluation of the template, we used our evaluation criteria in two independent groups: first using the 20 subjects that we used for the creation of the SUIT-N template and second, in a smaller group of 5 neonates (independent test subjects) that were not previously used on any of the procedures described in the methodology.

3. Results

3.1. Cerebellar isolation

Despite the low contrast, isolation of the cerebellum and brainstem was successful using our methodology. Fig. 1 shows the raw images (Fig. 1a and b) and the segmentation (Fig. 1c and d) of example subjects. While the final isolation mask was generally successful (Fig. 1e), in 24% of the cases there was some mislabeling of voxels, especially in the occipital cortex (Fig. 1f), which needed hand correction. Overall the isolation process takes approximately 3–5 min on a regular desktop computer.

3.2. Generation of the template

We generated a new Spatially Unbiased Infratentorial Neonatal (SUIT-N) Template following the nonlinear atlas generation algorithm described in the methods (Fig. 2). The spatial unbiasedness with respect to the UNC neonate template guarantees that the average coordinate of a cerebellar structure in the new template is the same as the average coordinate in the UNC template. In comparison to the adult cerebellar template (13), the neonatal template shows less details of the lobular organization. However, the main lateral trunks of the arbor vitae are clearly visible.

3.3. Evaluation

The average pair-wise correlation between images can be seen in Table 1. As expected, the linear whole-brain normalization (FSL FLIRT) led to the poorest overlap, with an average correlation of 0.78, while FSL FNIRT yielded a slightly higher correlation of 0.80 and SPM Normalize resulted in a correlation of 0.81. Our methods increased the pair-wise correlations to 0.97, with even the lowest correlation being higher than the highest obtained with the old methods. To ensure that these results do not solely reflect the fact that the template images represented the average geometry of those specific individuals, we validated the results with anatomical data from 5 independent subjects. The resulting anatomical correlations approximated those obtained from the atlas

Table 1
Evaluation of SUIT-N and whole-brain methods for the cerebellum.

Method	Atlas subjects			Independent test subjects		
	Cerebellar width (SD in mm)	Perimeter Location (SD in mm)	Voxel-wise correlation	Cerebellar width (SD in mm)	Perimeter location (SD in mm)	Voxel-wise correlation
FSL FLIRT	1.79	1.48	0.78	1.89	1.51	0.77
FSL FNIRT	2.21	1.45	0.80	1.98	1.46	0.83
SPM Normalize	1.37	1.12	0.81	1.43	1.09	0.83
SUIT-N	0.57	0.52	0.97	0.57	0.54	0.97

Cerebellar width and perimeter location values indicate the standard deviation [mm] across individuals after normalization. Voxel-wise correlation indicates the Pearson correlation between any pairs of aligned individuals. FSL-FLIRT, FSL-FNIRT, and SPM Normalize use the whole-brain UNC template. Each method was evaluated twice using the Atlas subjects ($n = 20$) and the independent test subjects ($n = 5$). See evaluation in the methods section.

group (Table 1), demonstrating the general applicability of the new method.

To provide a more precise evaluation of the anatomical overlap, we outlined the cerebellar perimeter on the individual cerebella. The cerebellar perimeter was substantially better aligned using SUIT-N than when using the whole-brain template (Fig. 3). The cerebellar width did not show dramatic differences between methods (55.6 mm in average), however, the standard deviation of the cerebellar width showed a reduction when using SUIT-N compared to the other methods. Similarly, the standard deviation of the perimeter location showed a reduction with SUIT-N (Table 1) i.e. the range of the average perimeter location for whole-brain linear was 6 mm, for the whole-brain nonlinear was 4 mm and for SUIT-N was 1.5 mm. Overall, the difference in the cerebellar perimeter was more variable when whole brain methods were implemented. SUIT-N reduced the variability to 68% compared to the linear normalization and 61% compared to the nonlinear normalization. Evaluation of the brainstem yielded similar results, with SUIT-N showing smaller standard deviation values in both metrics (Table 2).

Brainstem width and perimeter location values indicate the standard deviation [mm] across individuals after normalization. Voxel-wise correlation indicates the Pearson correlation between any pairs of aligned individuals. FSL-FLIRT, FSL-FNIRT, and SPM Normalize use the whole-brain UNC template. Each method was evaluated twice using the Atlas subjects ($n = 20$) and the independent test subjects ($n = 5$). See evaluation in the methods section.

4. Discussion

We have created the Spatially Unbiased Infra-Tentorial Neonatal (SUIT-N) template based on the anatomy of twenty healthy newborns. We have shown that our methodology outperforms whole-brain

normalization to the UNC template using either linear or nonlinear algorithms. This new tool will be essential for better diagnosis of cerebellar abnormalities during prenatal development.

Our isolation algorithm is a powerful tool that will aid clinicians in better understanding cerebellar development. In the current neonatal literature, clinicians typically perform manual delineation of the cerebellum (Allin et al., 2001; Limperopoulos et al., 2005; Peterson et al., 2000), a time-consuming task. The emergence of higher resolution MRI techniques makes this approach even more demanding. Our isolation algorithm segments and normalizes the cerebellum in under five minutes. In the cases that manual correction is necessary, an additional five minutes would be required to complete the process. Pediatric MRI is a growing field, and institutions and researchers are acquiring more data routinely. A reduction in processing time then becomes critically important in the analysis of such large clinical cohorts.

The second advance that our methodology provides is the normalization method. Using a whole-brain normalization induces inaccuracies into the normalization of cerebellar data. Here, we show that normalization using affine whole-brain normalization can lead to a variation of 6 mm in identifying a specific cerebellar location and 4 mm using a nonlinear approach. Considering this large spatial variation, it is easy to understand why many pediatric researchers have chosen to report total cerebellar volume rather than computing voxel-by-voxel volumetry (ten Donkelaar et al., 2003). SUIT-N provides a systematic way to accurately normalize the cerebellum, providing a means by which to identify volume difference at specific cerebellar locations, compare cerebellar lesions, and perform group analysis of functional activations in a standard space.

Currently, there is no gold-standard for an atlas template for neonates. As a reference coordinate system for SUIT-N, we used the UNC neonate template (Shi et al., 2011), which is widely adopted in the field.

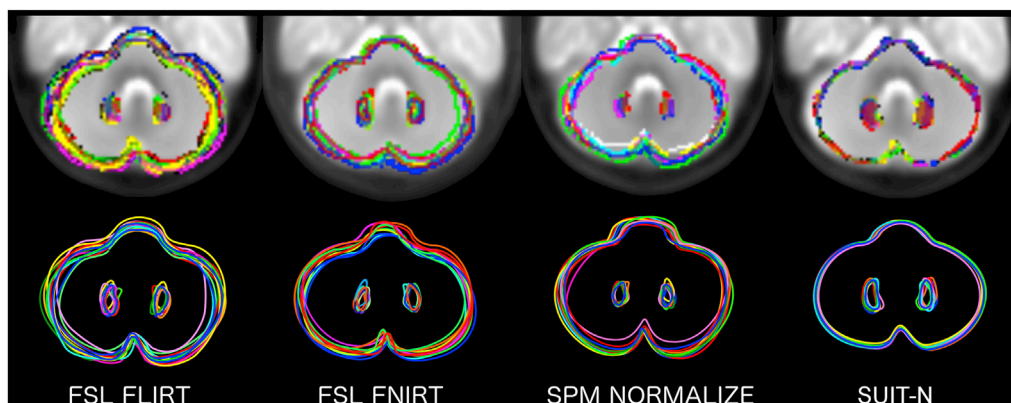


Fig. 3. Spatial distribution of the normalized cerebella. Overlap of the cerebellar diameter using whole brain linear (FSL FLIRT), nonlinear (FSL FNIRT and SPM NORMALIZE) and SUIT-N normalization. Top row shows the cerebellar perimeters of all individuals over the UNC neonate template using transparent overlapping, the lower row shows the same diameters using solid color lines.

Table 2
Evaluation of SUIT-N and whole-brain methods for the brainstem.

Method	Brainstem width (SD in mm)	Perimeter Location (SD in mm)	Brainstem width (SD in mm)	Perimeter location (SD in mm)
	Atlas subjects		Independent test subjects	
FSL FLIRT	1.81	1.03	1.83	1.02
FSL FNIRT	1.00	0.85	0.93	0.75
SPM Normalize	1.34	0.79	1.52	0.81
SUIT-N	0.87	0.55	0.95	0.58

If in the future, a novel atlas template is designated as an international standard by consensus, the cerebellar template can be easily adapted to a new coordinate system following the methods laid out here. In the same way, pediatric MRI acquisitions show a considerable variability in terms of resolution. Therefore, the toolbox is designed such that it can deal with images of any (also non-isotropic) resolution. However, we do not recommend the use of the toolbox with images that have a resolution lower than 1.5 mm in any dimension.

One limitation of our approach is the lack of white/gray matter contrast. Relative to other templates, SUIT-N has a better gray/white matter contrast, however the basic issue of the relatively weak myelination remains. Developments of new MRI protocols, combining different modalities such as magnetic transfer or water diffusion, could help to better delineate the different tissue types. In practice however, the acquisition of a T2-weighted image is often part of the standard clinical imaging protocol, and large amounts of data is available. For this reason, we decided to generate our template for this imaging contrast. Another important improvement that our toolbox might introduce in a future version is the possibility of performing longitudinal registration. This feature is relevant due to the high amount of change that the brain undergoes in the first year of life (Gao et al., 2015). This will be possible by creating intermediate templates based in a large cohort of data e.g. scans every three months. This approach will provide a smooth transition from the neonatal brain to the fully myelinated infant brain and hence a more accurate characterization of the developmental process.

SUIT-N is a software tool that did not previously exist in the pediatric MRI field. We hope it will be helpful in accelerating research into the important role of the cerebellum in healthy and atypical brain development.

Acknowledgments

The study was supported by the National Institutes of Health (RO1HL116585, IDDC, grant P30HD40677) to CL. CHC was supported by a postdoctoral award from the Brain and Mind Institute, as well as by a James S. McDonnell Scholar award to JD.

Appendix A. Supplementary data

Supplementary data to this article can be found online at <https://doi.org/10.1016/j.neuroimage.2018.09.048>.

References

- Allin, M., Matsumoto, H., Santhouse, A.M., Nosarti, C., AlAsady, M.H.S., Stewart, A.L., Rifkin, L., Murray, R.M., 2001. Cognitive and motor function and the size of the cerebellum in adolescents born very pre-term. *Brain* 124, 60–66. <https://doi.org/10.1093/brain/124.1.60>.
- Ashburner, J., Friston, K.J., 2005. Unified segmentation. *Neuroimage* 26, 839–851. <https://doi.org/10.1016/j.neuroimage.2005.02.018>.
- Diedrichsen, J., 2006. A spatially unbiased atlas template of the human cerebellum. *Neuroimage* 33, 127–138. <https://doi.org/10.1016/j.neuroimage.2006.05.056>.
- Diedrichsen, J., Maderwald, S., Küper, M., Thürling, M., Rabe, K., Gizewski, E.R., Ladd, M.E., Timmann, D., 2011. Imaging the deep cerebellar nuclei: a probabilistic atlas and normalization procedure. *Neuroimage* 54, 1786–1794. <https://doi.org/10.1016/j.neuroimage.2010.10.035>.
- du Plessis, A.J., Limperopoulos, C., Volpe, J.J., 2018. Cerebellar development. In: *Volpe's Neurology of the Newborn*. Elsevier, pp. 73–99. <https://doi.org/10.1016/B978-0-323-42876-7.00004-1>.
- Friston, K.J., Karl, J., Ashburner, J., Kiebel, S., Nichols, T., Penny, W.D., 2007. *Statistical Parametric Mapping: the Analysis of Functional Brain Images*. Elsevier/Academic Press.
- Gao, W., Alcauter, S., Elton, A., Hernandez-Castillo, C.R., Smith, J.K., Ramirez, J., Lin, W., 2015. Functional network development during the first year: relative sequence and socioeconomic correlations. *Cerebr. Cortex* 25. <https://doi.org/10.1093/cercor/bhu088>.
- Hashioka, A., Kobashi, S., Kuramoto, K., Wakata, Y., Ando, K., Ishikura, R., Ishikawa, T., Hirota, S., Hata, Y., Hashioka, A., Kobashi, S., Kuramoto, K., Hata, Y., Wakata, Y., Ando, K., Ishikura, R., Hirota, S., Ishikawa, T., 2012. A neonatal brain MR image template of 1 week newborn. *Int J CARS* 7, 273–280. <https://doi.org/10.1007/s11548-011-0646-5>.
- Kazemi, K., Moghaddam, H.A., Grebe, R., Gondry-Jouet, C., Wallois, F., 2007. A neonatal atlas template for spatial normalization of whole-brain magnetic resonance images of newborns: preliminary results. *Neuroimage* 37, 463–473. <https://doi.org/10.1016/j.neuroimage.2007.05.004>.
- Knickmeyer, R.C., Gouttard, S., Kang, C., Evans, D., Wilber, K., Smith, J.K., Hamer, R.M., Lin, W., Gerig, G., Gilmore, J.H., 2008. Development/plasticity/repair a Structural MRI Study of Human Brain Development from Birth to 2 Years. <https://doi.org/10.1523/JNEUROSCI.3479-08.2008>.
- Limperopoulos, C., Bassan, H., Gauvreau, K., Robertson, R.L., Sullivan, N.R., Benson, C.B., Avery, L., Stewart, J., MD, J.S.S., Ringer, S.A., Volpe, J.J., duPlessis, A.J., 2007. Does cerebellar injury in premature infants contribute to the high prevalence of long-term cognitive, learning, and behavioral disability in survivors? *Pediatrics* 120, 584 LP-593.
- Limperopoulos, C., Soul, J.S., Gauvreau, K., Huppi, P.S., Warfield, S.K., Bassan, H., Robertson, R.L., Volpe, J.J., du Plessis, A.J., 2005. Late gestation cerebellar growth is rapid and impeded by premature birth. *Pediatrics* 115, 688 LP-695.
- Peterson, B.S., Vohr, B., Staib, L.H., Cannistraci, C.J., Dolberg, A., Schneider, K.C., Katz, K.H., Westerveld, M., Sparrow, S., Anderson, A.W., Duncan, C.C., Makuch, R.W., Gore, J.C., Ment, L.R., 2000. Regional brain volume abnormalities and long-term cognitive outcome in preterm infants. *J. Am. Med. Assoc.* 284, 1939. <https://doi.org/10.1001/jama.284.15.1939>.
- Shi, F., Yap, P.-T., Wu, G., Jia, H., Gilmore, J.H., Lin, W., Shen, D., 2011. Infant brain atlases from neonates to 1- and 2-year-olds. *PLoS One* 6, e18746. <https://doi.org/10.1371/journal.pone.0018746>.
- Stoodley, C.J., Limperopoulos, C., 2016. Structure–function relationships in the developing cerebellum: evidence from early-life cerebellar injury and neurodevelopmental disorders. *Semin. Fetal Neonatal Med.* 21, 356–364. <https://doi.org/10.1016/j.siny.2016.04.010>.
- ten Donkelaar, H.J., Lammens, M., Wesseling, P., Thijssen, H.O., Renier, W.O., 2003. Development and developmental disorders of the human cerebellum. *J. Neurol.* 250, 1025–1036. <https://doi.org/10.1007/s00415-003-0199-9>.
- Triulzi, F., Parazzini, C., Righini, A., 2005. MRI of fetal and neonatal cerebellar development. *Semin. Fetal Neonatal Med.* 10, 411–420. <https://doi.org/10.1016/j.siny.2005.05.004>.
- Volpe, J.J., 2009. Cerebellum of the Premature Infant: Rapidly Developing, Vulnerable, Clinically Important. <https://doi.org/10.1177/0883073809338067>.
- Woodward, L.J., Anderson, P.J., Austin, N.C., Howard, K., Inder, T.E., 2006. Neonatal MRI to predict neurodevelopmental outcomes in preterm infants. *N. Engl. J. Med.* 355, 685–694. <https://doi.org/10.1056/NEJMoa053792>.